Soil Moisture Determination using Satellites

N. T. Nxumalo[1], G. G. S. Pegram[1]

[1] Department of Civil Engineering, University of KwaZulu-Natal, DURBAN, 4014

Abstract

The amount of water in the soil acts as a vital switch between atmosphere and ground, governing many Earth-bound water processes: infiltration, evapotranspiration, interflow and ground-water recharge. Soil moisture (SM) is painfully difficult to measure and is therefore seldom used explicitly in hydrological modelling, even though modern distributed models implicitly demand it. If accurate spatial estimates of SM over large areas were available, they would be useful in many applications in Hydrology and Meteorology, besides Agriculture. It is because of its importance in these areas, that huge international effort is being made to use remote sensing to estimate SM at increasingly finer resolution.

The purpose of this paper is to highlight the work that has already been done at UKZN, using a recently acquired direct satellite data link with EUMETSAT, to "prepare the ground" in RSA, via a WRC Consultancy in 2005: K8/598 "In Connection with Soil Moisture Mapping from Satellites"

Keywords: *Brightness temperature, soil moisture, temperature gradient, evapotranspiration.*

1 Introduction

Soil moisture significantly influences weather and climate, having a pronounced effect in the control of near surface exchanges of water and energy. The interaction between soil moisture, evapotranspiration and precipitation, the three core variables of the soil-vegetation-atmosphere water exchange system, determine the partitioning between infiltration and runoff. Soil moisture, as a result, is of great significance in a number of disciplines such as agriculture, hydrology, meteorology and disaster management.

From the agronomist's point of view, plant growth can be adversely affected by either too little or too much water, although usually the former. The hydrologist's and disaster manager's interests are that excess soil moisture can lead to large runoffs and streamflows resulting in floods while soil water deficits can aggravate a hydrological drought.

In meteorology and climate change studies soil moisture is important because it directly affects the partitioning of energy at the surface between latent and sensible heating. Modelling studies show that strong perturbations in soil moisture on global and regional scales can affect atmospheric circulation, and may persist for several months (Dirnmeyer and Shukla, 1993).

2 Soil Moisture Measurements

Soil moisture is a parameter with great spatial and temporal variability. It is because of these properties that measurement techniques are to be carefully planned. Consideration of the intended application is also vital in deciding the measurement technique.

2.1 Field (Point) Measurements

Field measurements are the considered the 'traditional' methods for measuring soil moisture. These are essentially point measurements and are locally accurate. There are various field measurement techniques employed, of which two will be briefly discussed, namely the thermo-gravimetric and the Time-Domain Reflectometry (TDR) method. Other measurement devices include capacitance probes, resistance probes, neutron probes, and tensiometers.

The thermo-gravimetric method consists of removing a soil sample and by determining its weight before and after it has been dried in an oven at 105 ºC for 24 hours (Hillel, 1980). The thermo-gravimetric is the standard method for soil wetness determination on which all other methods are ultimately calibrated (Schulin et al., 1992). A point worth noting about this method of soil moisture determination is that it is destructive; hence samples cannot be taken from the same point on subsequent sampling dates.

In the Time-Domain Reflectometry (TDR) method the velocity of propagation of a high frequency voltage pulse in the soil is measured and related to the soil dielectric properties. Since the dielectric constant of a soil increases with the water fraction the soil moisture content can be estimated (Topp, 1992).

One problem associated with these 'traditional' measurement techniques is that they are point-based measurements and they do not address the spatial variability of soil moisture. These methods also tend to be labour intensive and can thus prove costly especially in dense networks.

2.2 Hydrological Models

With the numerous difficulties presented in estimating the spatial distribution of soil moisture by point measurements, hydrological models are often used. Soil moisture models are used in the prediction of the spatial variation of soil moisture profiles. However, these models tend to require considerable amounts of meteorological data, which most of the time proves either difficult or costly to obtain (Ottlé and Vidal-Madjar, 1994). Moreover, the various parameters are quite difficult to determine, requiring calibration and often resulting in simulation errors, as experienced by Wood et al., 1993.

2.3 Soil Moisture Measurement Using Remotely Sensed Data

By playing such a pivotal role in meteorology and hydrology, soil moisture is continuing to attract more and more interest in developing methods to assess and observe this parameter by means of remote sensing. Remote sensing is, broadly speaking, the collection of information about an object without coming into physical contact with it (Rees, 1990). Since the launch of the ERTS-A satellite in July 1972, which was later renamed Landsat 1, there have been numerous launches of space borne sensors operating in the visible, infrared and microwave range of the electromagnetic spectrum.

Remote sensing was soon perceived as a favorable contender in solving the problems associated with traditional methods for measuring soil moisture. Firstly, it would naturally provide areal measures of soil moisture rather than point data. Secondly, soil moisture maps of large regions could be produced at relatively low monetary and time costs. As a result, substantial effort has been put into the development of remote sensing techniques for soil moisture retrieval. Remote sensing techniques offer the potential to address both the problems of spatial and temporal variability of soil moisture.

However, remote sensing techniques have the following drawbacks:

- Soil moisture measurements by remote sensing tend to be limited to the top layers of the earth surface (up to 5cm depth).
- These techniques are adversely affected by the presence of vegetation cover, surface roughness and topography.

Soil moisture measurements by remote sensing are done with the aid of two types of satellites:

- Polar-orbiting satellites
- Geostationary satellites

The key differences between these two types of satellites are great; they have different measurement devices, orbit properties, observation repeat cycles and resolutions (both spatial and temporal). Geostationary satellites are satellites that are stationary relative to the earth. These satellites revolve around the earth in a period of 24 hours. Geostationary satellites are further away from the earth with orbits at about 30 000 km above the earth's surface. Imaging done with these satellites is hence at a coarser resolution than that done using polar orbiting satellites. Although most studies focus on the measurement of SM using microwave sensors (the common instrument on polar orbiters) sensors operating in the visible and infrared (common to geostationary satellites) can provide some information about soil moisture patterns. This is because soil colour and surface temperatures are influenced by soil wetness, making the use of thermal infrared and visible spectrum imagers in SM measurement another SM estimation possibility.

For applications in flash flood forecasting, soil moisture changes need to be monitored at high temporal resolution and over large spatial extents. It is for this reason that geostationary satellites are preferred in that context. The main advantage of geostationary satellites is the shorter observation repeat cycle (i.e. time between successive observations) on a particular patch of ground (for geostationary satellites, the period is between 15 and 30 minutes compared to the repeat cycles of up to 35 days for polar orbiters). This property of geostationary satellites best addresses the temporal variability of soil moisture since the soil surface may change from dry to wet within a period in the order of hours and the top few centimeters are the most exposed to the atmosphere and exhibit the most rapid changes in soil moisture content in response to evaporation and rainfall (Raju *et al.*, 1995; Capehart and Carlson, 1997) with the soil moisture content in the deeper layers changing more slowly.

For the SM mapping currently being undertaken in the University of KwaZulu-Natal's Satellite Application and Hydrometeorology Group (UKZN-SAHG), the data stream from EUMETSAT's METEOSAT-8 (also known as METEOSAT Second Generation, or MSG) is used.

3 METEOSAT Second Generation (MSG)

The first of EUMETSAT's Second Generation satellites, MSG, is already in use and positioned in geostationary orbit above 0° longitude and 0° latitude. MSG is able to generate multi-spectral imagery of the Earth's surface and cloud systems at double the rate (every 15 minutes instead of every half an hour) of its predecessor.
The type of instrumentation onboard the MSG satellites is the Spinning Enhanced Visible and Infrared Imager – SEVIRI, a 12 channel imager compared to the three channels from the previous METEOSATs. There is also a vastly improved geometrical resolution (1 km for the high-resolution visible channel and 3 km for the other channels).

Table 1 gives a description of the channels and their intended use. The derived surface properties are for cloud free areas with a view at nadir.

Table 1. Surface Properties From MSG Channels

Channel	Spectral Range	Main Surface Properties (for cloudfree areas, NADIR viewing)
01 (VIS 0.6)	Visible	surface reflectivity (albedo) at 0.6 μm
02 (VIS 0.8)		surface reflectivity (albedo) at 0.8 μm, "greeness" of vegetation
03 (NIR 1.6)	Near Infrared	surface reflectivity (albedo) at 1.6 μm
04 (IR 3.9)	Infrared	Day-time: surface temperature, surface reflectivity (albedo) at 3.9 μm, surface emissivity Night-time:surface temperature, surface emissivity
05 (WV 6.2)	Water Vapor	upper-level moisture
06 (WV7.3)		mid-level moisture
07 (IR 8.7)	Infrared	surface temperature, surface emissivity, humidity
08 (IR9.7)		surface temperature, ozone content
09 (IR 10.8)		surface temperature
10 (IR 12.0)		surface temperature, humidity
11 (IR13.4)		surface temperature, lapse rate between surface and 800 hPa
12 (HRV)	High Res. Visible	surface reflectivity (albedo, broadband 0.4 - 1.1 μm)

Most of these products are still under development by the various Satellite Application Facilities (SAF), which are specialised development and processing centres.

3.1 Soil Moisture from MSG

There is currently no available method that measures SM directly from MSG. All the currently available remote sensing techniques measure SM through indirect means. Studies have shown that the rate of heating of the land is strongly controlled by the availability of soil water or lack thereof. The land surface skin temperature state has principal control on land-atmosphere fluxes of water and energy. It is closely related to soil water states, and is easily observable from space and aircraft infrared sensors in cloud-free conditions. The SEVIRI instrument, using the infrared (IR) channels 9 and 10 (wavelengths 10.8μm and 12.0μm respectively), measures the brightness temperature, T_B, which in turn, using a conversion algorithm, is converted into land surface temperature.

3.1.1 The SEBAL Algorithm

One such algorithm is the Surface Energy Balance Algorithm for Land (SEBAL) developed by Bastiaanssen et al. (1998a,b). SEBAL consists of a suite of algorithms to solve the complete energy balance for each pixel in a satellite brightness temperature, T_B, image. The basic SEBAL equations are given in the sections that follow. A schematic representation of the parameters and steps required in the SEBAL algorithm is shown in Figure 1.

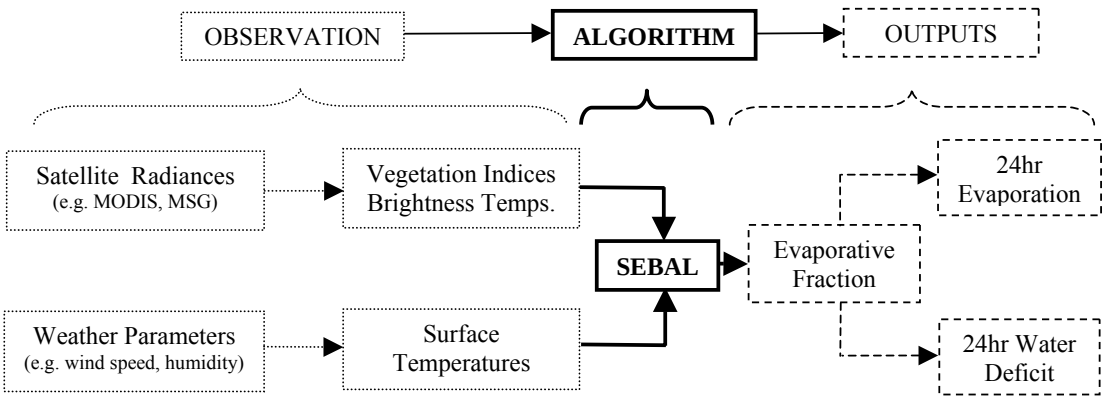

Figure 1. Schematic Illustration of the Steps Involved in ET Estimation

As no method exists that measures SM directly, most methods (including the SEBAL method) make use of the fact that SM and evaporative fraction (defined by equation (4)) are strongly correlated. An example of such a relation is shown in Figure 2.

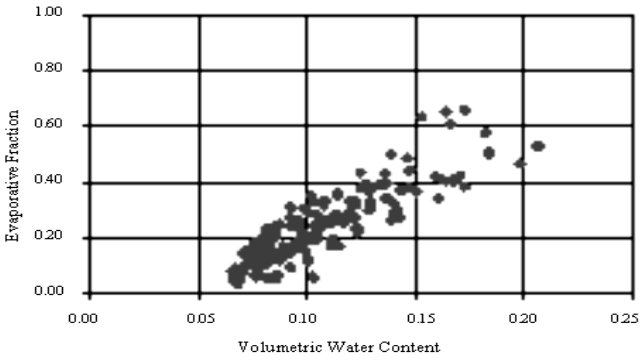

Figure 2. Evaporative Fraction vs. Soil Moisture for Sevilleta, New Mexico (taken from Bastiaanssen et al., 2000)

Therefore, we can determine regional soil moisture (% saturation) distribution using the latent heat flux (i.e evapotranspiration) and sensible heat flux determined by SEBAL.

Reviewing the literature related to the assessment of the evapotranspiration and of the surface fluxes is outside the scope of this paper; only some broad assessments will be made. Interested readers can refer for instance to Carlson (1986), Choudhury (1994), Kustas and Norman (1999) to find a general description and discussion of remote sensing approaches in this field.

As explained by (Bastiaanssen et al., 2000) Latent heat flux, LE, is usually deduced from the surface energy balance equation:

$$R_n - LE - H - Q_g = 0 \tag{1}$$

given that the other terms of the equation are known. R_n, the net radiation, includes the contributions from the short and long wave radiation fluxes and is given as follows:

$$R_n = (1-r)K_d + L_d - L_u \tag{2}$$

where r is the albedo, K_d the visible irradiance (global, downward, solar radiation flux), L_d the infrared irradiance downward (infrared radiation flux emitted by the atmosphere) and L_u the infrared exiting radiation (upward infrared radiation flux emitted and reflected by the surface). Q_g, is the heat conduction flux into the ground, often neglected at the daily time step, or is assumed to be a constant proportion of the net radiation for shorter time steps.

The sensible heat flux, H, may be expressed by the bulk aerodynamic method as:

$$H = \rho * c_p * \frac{(T_s - T_a)}{r_a} \tag{3}$$

where ρ is the air density, c_p its specific heat at constant pressure, T_s the surface (aerodynamic) temperature, T_a an air temperature higher in the atmospheric surface layer and r_a an aerodynamic resistance coefficient depending on several parameters (the atmospheric stability, the roughness of the surface, the friction velocity, etc.). The variables R_n and T_s are estimated from satellite data, and T_a and r_a from ground based meteorological measurements.

With the sensible and latent heat known per pixel, the evaporative fraction, f, can thus be calculated as follows:

$$f = \frac{LE}{R_n - Q_g} \tag{4}$$

Through using these basic equations SEBAL can be used to determine SM. However, although it is useful for specifying the interactions between the variables, the SEBAL algorithm was found to be rather complicated and unsuitable for real time determination of SM.

4 Current Status of SM Estimation at the UKZN-SAHG

Numerous studies (e.g. Hillel, 1980 and Portmann et al., 2004.) have shown the surface heating rate, referred to as the temperature gradient, is related to the soil moisture state. The rate of increase in temperature within a specified time period is not constant throughout a day (higher in the morning than at mid day), thus brightness temperature data are captured between 0800hrs and 1000hrs local time.

For an area covering a major part of southern Africa (south of 20°S), the UKZN-SAHG is archiving the imagery from the IR channels 9 and 10 (wavelengths 10.8µm and 12.0µm respectively) for every square 1 minute of arc, from 0800 to 1000hrs local time at ¼ hour intervals. Using these data, it is intended to link the variations of brightness temperature and heating rates to SM.

A study area encompassing the Liebenbergsvlei catchment was chosen. The area is rectangular, measuring 120 by 60 minutes of arc. The top left corner of the site, labeled 'C' in Figure 3, is located at 27º 50' 00" E and 27º 00' 00" S.

This site was favored as a test site because it is well instrumented and has had numerous hydrologically based investigations carried out on it. All relevant physical data are also readily available. This includes the digital elevation model (DEM), obtained from the UKZN School of Bio-resources and Engineering Hydrology; WR90 soil types maps from the Water Research Commission and land cover maps, available for download from the United States Geological Surveys (USGS) website.

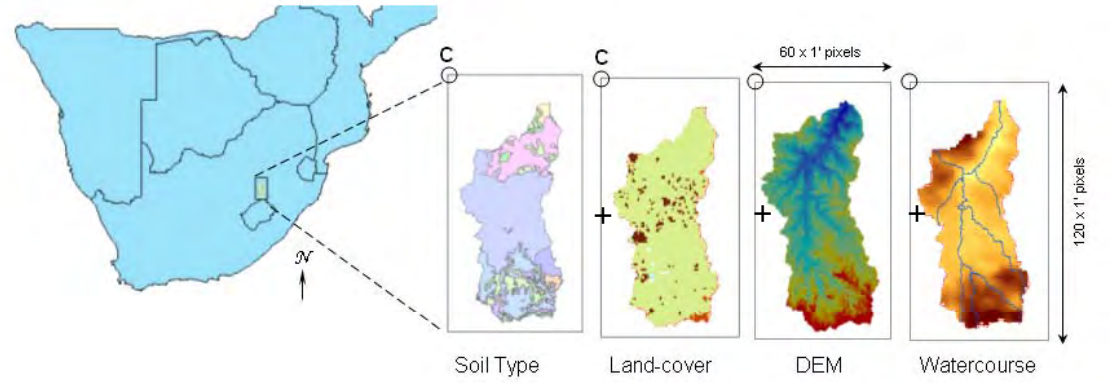

Figure 3. UKZN-SAHG's Test Area and the Available Data

4.1 Data Acquisition at the UKZN-SAHG

The UKZN-SAHG now receives MSG data from all 12 channels via the EumetCast system, installed only recently in May 2005, every 15minutes. Figures 4 a) and b) show the setup which includes a 2.5m receiving dish and two computers: one for receiving data and the other to process it.

Figure 4. (a) The 2.5m Dish on Top of Civil Eng. Department (UKZN-Durban) and (b) Receiving and Processing Station

4.2 Data Processing at the UKZN-SAHG

From the two IR channel images, preliminary investigations into the effects of the various soil conditions have begun. This includes the observation of temperature gradients across the test area and the effects of wetness on the brightness temperature gradient plots. A typical IR image for southern Africa is shown in Figure 4.

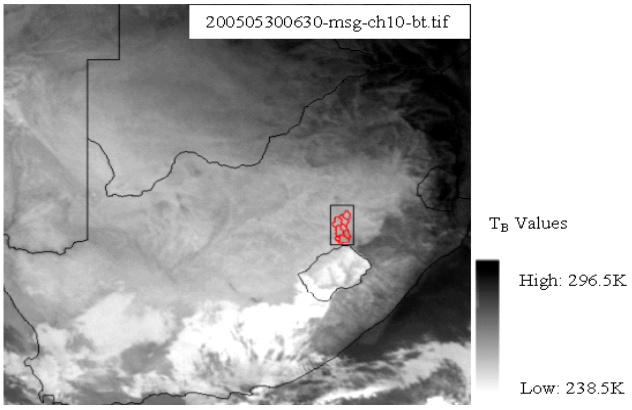

Figure 4. IR Image taken from MSG Channel 10 at 0830hrs Local Time on May 30, 2005

The image in Figure 4 shows brightness temperatures in °K. The darker shades represent warmer surfaces and the white on the southern part of the image is mostly cloud, hence cold.

For the preliminary investigations, the IR 10.8μm (MSG channel 9) data were used. This is because, of the six available IR channels on MSG, this one is least affected by atmospheric effects. Firstly, a general behavior of the soil with respect to heating rates was investigated. This was achieved by processing images taken every quarter hour between 0800hrs and 1000hrs local time. From these images, the general heating pattern for the test was observed qualitatively. The images for the 2 hour period are shown in Figure 5.

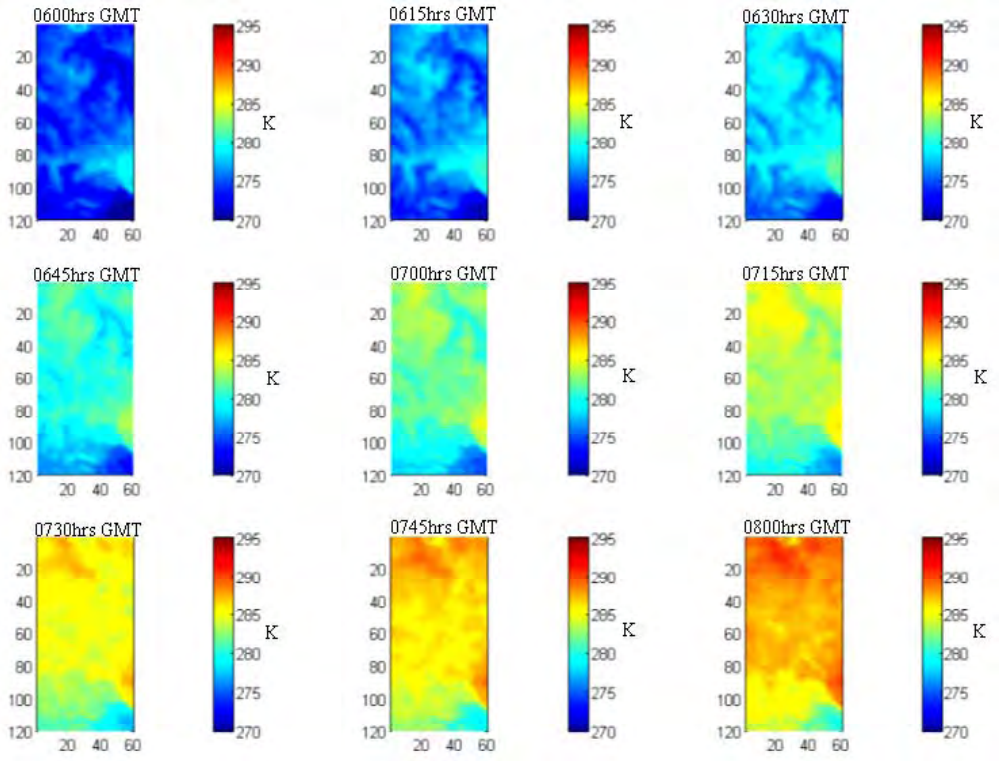

Figure 5. Brightness Temperature Plots at Quarter Hourly Intervals between 0800 and 1000 hrs Local Time on May 30, 2005

4.2.1 Observations from Brightness Temperature (T_B) Plots

From the series of T_B plots, it was noted that there is a discernible outline of the valleys and possibly watercourses. This is because of the temperature difference between the valleys starting off colder than the higher ground. Also, it is worth noting that the ground at high altitude starts off with almost the same temperature gradient as the valleys but as time progresses, the valleys heat up at a much higher rate by 1000 h their temperatures tend to 'level' out at the surrounding maximum temperature. This implies that the earlier gradients at each pixel are mutually more consistent over the area, implying that their relative SM content is similar. The suggestion is that the critical gradients should be measured between 0800 and 0900 local time. Following this idea, a visual representation of the spatial variation of the temperature gradient in a 3-D plot of the total temperature change within the first hour of observation is shown in Figure 6. The maximum change tends to occur in the low-lying areas shown in Figure 3.

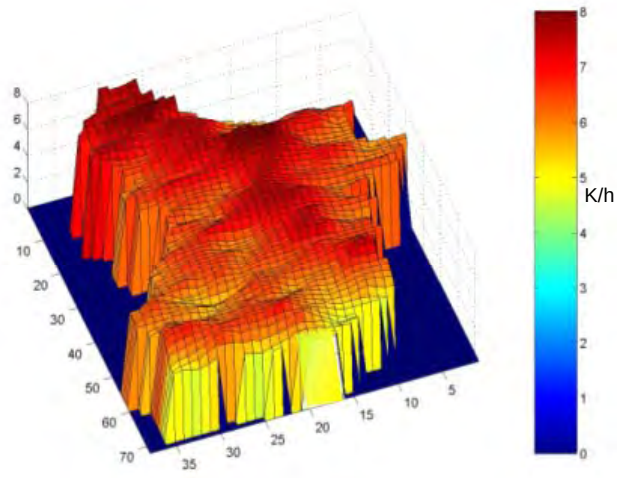

Figure 6. 3-D T_B Gradient Plot (ºK/h) for the Liebenbergsvlei Catchment on 30-05-05

To make this comparison clearer, the section of river that runs through the Liebensbergvlei was overlaid onto the brightness temperature plots, as shown in Figure 7. The image chosen was the 0630hrs GMT image because this was the temperature plot in which the valley features were more pronounced.

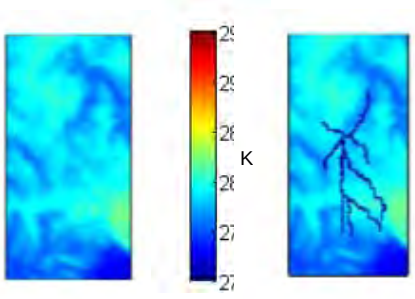

Figure 7. Plots of T_B at 0630hrs GMT (a) Before River Overlay (b) After River Overlay

Having made these observations, the behavior of the temperature gradient with time and position was also investigated. In order to get a feel of the time variation of the temperature, the mean temperature over the test site (120 x 60 pixels) observed by MSG at 15 minute intervals was plotted against time, as shown in Figure 8.

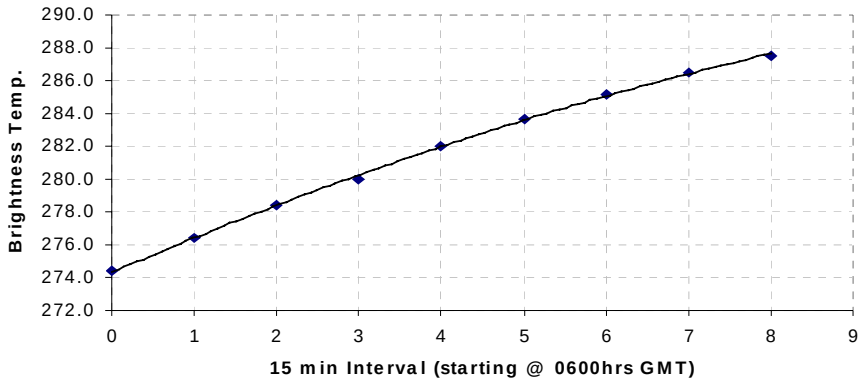

Figure 8. Plot of mean (over the test area) of Brightness Temperature, T_B, vs. Time

From the plot shown in Figure 8, it can be noted that the mean brightness temperature gradient is nearly constant over the first hour, and then gradually decreases after that.

From this plot, however, only the overall trend in temperature gradients across the test area can be observed. This plot does not take into account the heterogeneity of the soil condition per pixel. So, temperature variations at each pixel lying on a line across the test site (60 pixels: see the line A-A in Figure 9 (a)) were calculated and plotted for each ¼ hour interval and shown in Figure 9 (b).

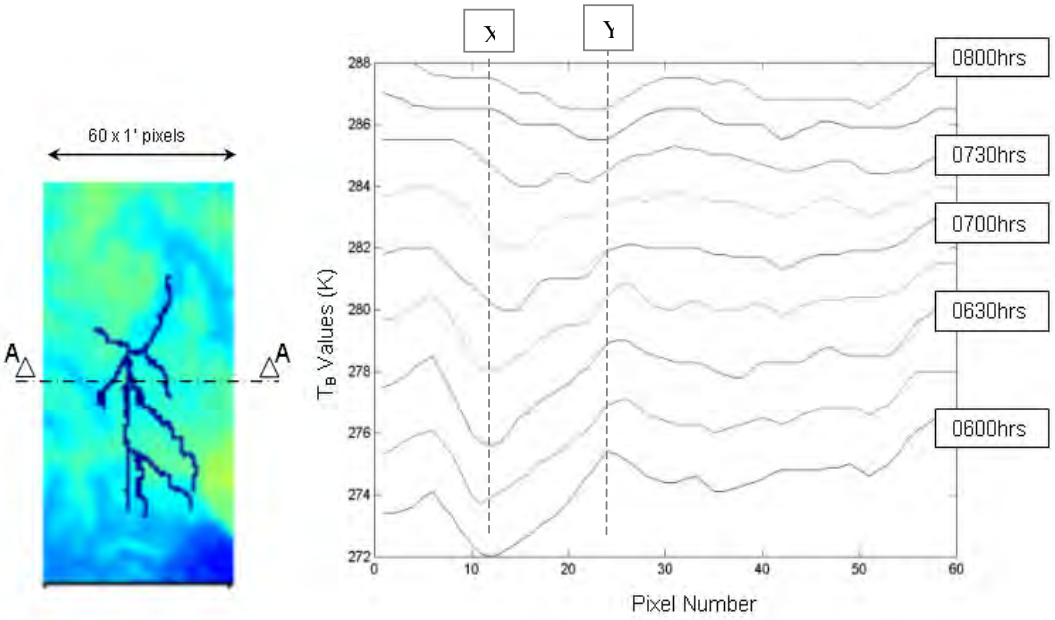

Figure 9. (a) Cross Section Position and (b) Quarter Hourly T_B Plots For Each of 60 Pixels (Times Shown are GMT)

The plot shown in Figure 9 (b) illustrates the response of each pixel to heating. This plot also shows that the temperature range starts off quite large and gradually diminishes with time. The differential heating rate for valley and high ground locations can be best shown using a plot such as that in Figure 10. For illustration purposes, two kinds of pixels were chosen: one initially 'cold' pixel (denoted as 'X') and one initially 'warm' pixel (denoted as 'Y'), whose locations are indicated by the dashed lines in Figure 9 (b).

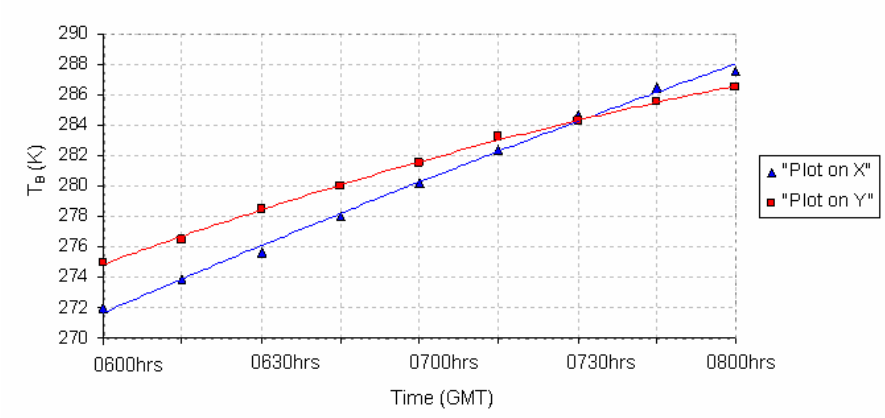

Figure 10. Brightness Temperature Plots for Pixels 'X' and 'Y'

Considering the fact that the test area has an almost homogeneous land cover and soil type along the line A-A (see Figure 3), it can be assumed that the difference in heating rates is due to either the location of the pixel (i.e. altitude or topography) or SM condition. The behavior of the two pixels cannot be described only in terms of SM content but rather in also terms of topographical location. The Liebensbergvlei is known to be an area with hills and valleys, hence there is a high possibility of mountain shading for some areas thus causing a rather uneven heating of the various pixels.

Also, this plot shows that there is a low noise level at pixel scale. That is, the temperature changes follow a uniform trend which is an encouraging characteristic of the MSG image.

5 Problems Encountered and Possible Future Work

Although the land surface temperature product is not yet available from the relevant Land-SAF, the investigations carried out by the UKZN-SAHG over a relatively short period of 8 months have revealed some problems among the encouraging signs. From this experience and a subsequent search of the literature, possible means of solution have been considered and listed.

5.1 The Effect of Cloud Cover on Determination of T_B

One of the known disadvantages of the use of spectral and IR imagery in the remote sensing of SM is the presence of cloud cover. This tends to affect the estimation of T_B and thus needs to be resolved. One way of getting around this problem would be to put into place a precise method of cloud detection. This could then be used as a time varying cloud mask i.e. the areas affected by cloud could be marked as having no data rather than getting a misleading cloud top temperature value.

Cloud masking is relatively easy to develop because the detection of various cloud forms is a feature made possible by the capabilities of the SEVIRI instrument on MSG. Cloud detection cannot however be done using only one channel. This is because different types of clouds respond differently to the various wavelengths. For example, the detection of thin ice clouds using a single channel is quite difficult but this is much easier using an image created from the subtraction of the signal of the IR12.0μm channel from that of the IR10.8μm channel. Hence sometimes numerous channels have to be used at once in what is known as a Red-Green-Blue combination, such as shown in Figure 11.

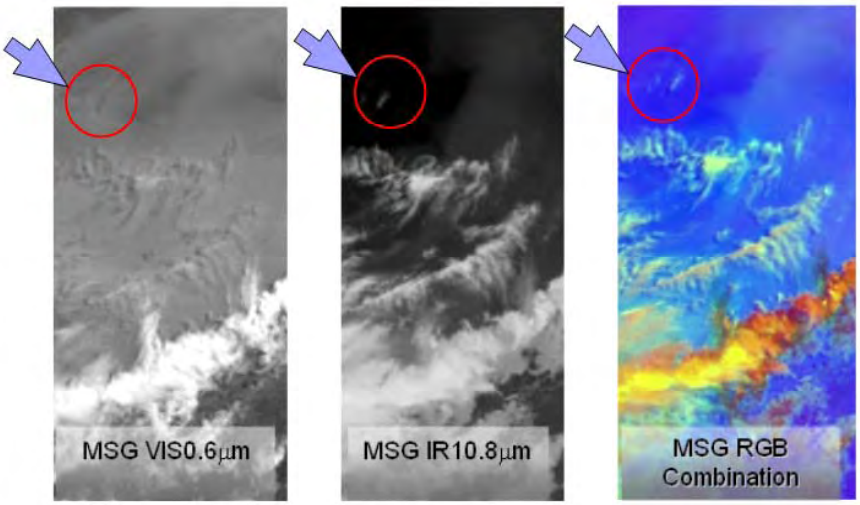

Figure 11. The Thin Clouds Detection using MSG

The thin clouds are barely discernible in the individual channels but more evident in the RGB image. The RGB image was created using the following RGB combinations:

R = WV6.2 - WV7.3
G = IR3.9 - IR10.8
B = NIR1.6 - VIS0.6

5.2 The Effect of Season on Heating Rates

Due to the fact that solar angles vary according to season as well as time of day, it is important to note that the sun's position exerts a huge influence on heating rates. That is, for the same geographical location at 0630hrs GMT in winter, the sun is at a different angle compared to the same time in summer. This actually makes it necessary that alternative methods of determining the heating rate be investigated. One way of achieving better results, would be to determine the precise sunrise time for the particular location and use the temperatures at that time as initial soil temperatures. This however does not solve the problem entirely because depending on the season, the sun stays longer above particular angles. Instead of determining the heating rate as the temperature difference within a fixed time interval, the heating rate can be better determined as the temperature change between particular solar angles, to be determined.

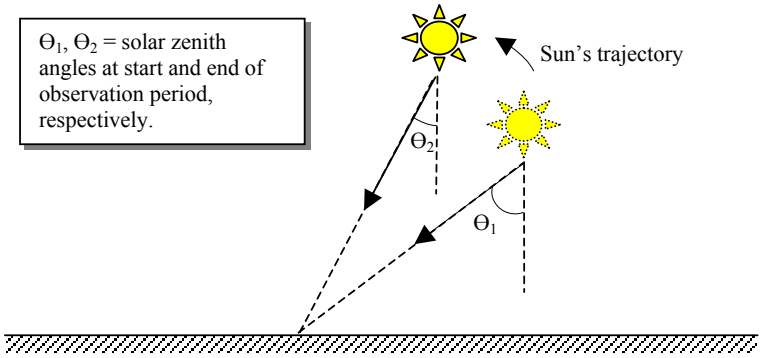

Figure 12. Temperature Observation between Solar Zenith Angles

According to Portmann et al. 2004, the heating-rate or temperature difference normalised by incoming (short-wave) radiation gives a better representation than temperature differences over fixed time periods. For normalisation, the cosines of the sun zenith angle (SUZ) are usually taken. This idea is to be exploited further.

6 Summary and Conclusion

This paper summarises the work in progress that has already been achieved during the last 8 months at UKZN-SAHG and indicates the potential usefulness of remote sensing in SM determination.

References

Bastiaanssen, W.G.M., Cleverly, J., Hendrickx, J.M.H., Hong, S., Neville, P., Small, E. and Woolslayer, J. 2000. Regional Distribution Of Soil Moisture in the Middle of the Rio Grande Basin.

Bastiaanssen, W.G.M., Menenti, M., Feddes, R.A., Holtslag, A.A.M. 1998. A Remote Sensing Surface Energy Balance Algorithm for Land (SEBAL) 1. Formulation, J. Hydrol. 212; 213. 198–212.

Capehart, W. J., and Carlson, T. N. 1994. Estimating Near-Surface Soil Moisture Availability Using a Meteorologically Driven Soil-Water Profile Model. J. Hydrol., 160: 1-20.

Carlson, T.N. 1986. Regional-scale estimates of surface moisture availability and thermal inertia using remote thermal measurements, Remote Sens. Rev. 1. 197–247.

Choudhury, B.J. 1994. Synergism of multispectral satellite observations for estimating regional land surface evaporation, Remote Sens. Environ. 49 264–274.

Choudhury, B.J., Idso, S.B., Reginato, R.J. 1987. Analysis of an empirical model for soil heat flux under a growing wheat crop for estimating evapotranspiration by an infrared-temperature based energy balance equation, Agric. For. Meteorol. 39 283–297.

Hillel, D. 1980. Introduction to Soil Physics, Academic Press, San Diego, p.365.

Kustas W.P., Daughtry C.S.T., Van Oevelen P.J. 1993. Analytical treatment of the relationships between soil heat flux/net radiation ratio and vegetation indices, Remote Sens. Environ. 46. 319–330.

Kustas W.P., Norman J.M. 1999. Evaluation of soil and vegetation heat flux predictions using a simple two source model with radiometric temperatures for partial canopy cover, Agric. For. Meteorol. 94. 13–29.

Norman J.M., Divakarla M., Goel N.S. 1995. Algorithms for extracting information from remote thermal-IR observations of the Earth's surface, Remote Sens. Environ. 51. 157–168.

Ottlé, C., Vidal-Madjar, D. 1994. Assimilation of Soil Moisture Inferred from Infrared Remote Sensing in a Hydrological Model Over the HAPEX-MOBILHY Region, Journal of Hydrology, 158: 241-264

Portmann, F., Wagner, W., and Scipal K. 2004. Evaluation of Early Morning Heating Rate-derived Soil Moisture in Southern Europe. EUMETSAT Land SAF.

Raju, S., Chanzy, A., Wigneron, J., Calvert, J., Kerr, Y., and Laguerre, L. 1995. Soil Moisture and Temperature Profile Effects on Microwave Emission at Low Frequencies. Remote Sens. Environ., 54: 85-97.

Schulin, R., Flühler H., Selim, H. M., Sevruk, B., Wierenga, P. J. 1992. Soil Moisture, Part III, In Snow Cover Measurements and Areal Assessment of Precipitation and Soil Moisture, edited by B. Sevruk, WMO, Operational Hydrological Report, No. 55, pp. 219-283.

Topp, G. C. 1992. The measurement and Monitoring of Soil Water Content by TDR, in Soil Moisture Modelling, Proceeds of National Hydrology Research Centre Workshop, March 9-10, 1992, Saskatoon, Saskatechewan, Canada, pp. 155-161.

Wood, E. F., Lin, D. S.; Mancini, M., Thongs, D. J., Troch, P. A., Jackson, T. J., Famiglietti, J. S. and Engman, E. T. 1993. Intercomparison Between Passive and Active Microwave Remote Sensing and Hydrological Modeling for Soil Moisture. Advances in Space Research, 13(5): 167-176.